# An Efficient Two-Dimensional FDTD Method for Bio-Electromagnetic Applications

Rui Qiang[1], Dagang Wu[1], Ji Chen[1], Shumin Wang[2], Donald Wilton[1], and Wolfgang Kainz[3]

[1]Department of Electrical and Computer Engineering, University of Houston, Houston, TX, 77204 USA
[2]National Institutes of Health, Bethesda, MD 20892 USA
[3]U.S. Food and Drug Administration, Center for Devices and Radiological Health (CDRH), Rockville, MD 20852 USA

**We propose an efficient algorithm for the simulation of densely sampled biological objects. This technique is based on an algebraic multi-grid (AMG) accelerated Crank-Nicholson (CN) finite-difference time-domain (FDTD) method. Using this scheme, simulation time step sizes are no longer limited by the Courant-Friedrich-Levy (CFL) number. A practical guideline on how to choose appropriate time-step sizes for accurate bioelectromagnetic applications is also presented. Numerical examples are used to demonstrate the effectiveness of this technique.**

*Index Terms*—**Algebraic multi-grid method, bio-electromagnetics, FDTD method, unconditionally stable algorithm.**

## I. Introduction

THE interaction between electromagnetic waves and biological tissues has received renewed attention recently due to the increased clinical applications of magnetic resonance imaging (MRI) procedures and the extensive usage of cellular phones [1], [2]. To model such interactions, computational electromagnetic techniques have often been used. Among these numerical methods, the FDTD method has proven to be an effective technique. It has been successfully applied in cellular phone antenna designs and MRI system developments [2], [3].

However, this algorithm's efficiency begins to decrease when biological objects need to be modeled using very high resolution [4]. For this kind of application, the FDTD method requires a large number of iterations since the algorithm's time step size is limited by the minimum segment size in the spatial discretization [4]. For example, to simulate the interaction between electromagnetic fields and a two-dimensional (2D) 2 mm resolution human head model, the maximum time-step size can be used is 4.71 picoseconds. If we need to obtain the B1 fields distribution generated by a 1.5 T (64 MHz) MRI radio frequency (RF) coil, over 10 000 FDTD iterations are required.

To improve the computational efficiency of the FDTD method, some post-processing techniques, such as signal processing methods and the frequency scaling approaches [5] [6], have been used. These techniques have shown some improved efficiency in FDTD simulations; however, they are often limited to specific applications and may not be applied to general bio-electromagnetic simulations. Recently, an alternating-direction-implicit (ADI) FDTD method has been proposed [7]. In this technique, the simulation time step size is no longer limited by the CFL stability condition and yet has very low computational overhead. If one can use larger time step size than that of the conventional FDTD method, the total iteration number in ADI-FDTD method can be reduced. This could lead to an overall reduced CPU time than that of the conventional FDTD method.

However, truncation error associated with this method can become very large for many practical applications [8], [9]. Further analysis has shown that errors in ADI-FDTD simulations result from the splitting procedure in the ADI-FDTD formulation [8], [9]. Alternative choice is to use the unconditionally stable Crank-Nicholson (CN) algorithm that does not suffer from the splitting error. However, this algorithm requires one to solve a band-limited matrix during each time step, which is computational expensive [10]. If the computational overhead associated with solving the CN-FDTD method is too high, it may out-weight the advantage of using larger time step sizes.

To improve the computational efficiency associated with solving these band-limited matrices, we proposed a multi-grid technique. This approach allows us to have very low computational overhead and yet retains a high level of accuracy for low frequency bio-medical applications.

The remainder of this paper is organized as follows. Section II describes the development of the algorithm and its accuracy analysis. Section III demonstrates the accuracy and effectiveness of this algorithm via numerical examples and Section IV concludes the paper.

## II. Methodology

### A. CN-FDTD Formulation

To illustrate this method, we use 2D transverse magnetic (TM) case as an example. Similar derivation can be obtained for the transverse electric (TE) case. For the 2D TM case, the Maxwell's equation can be expressed as

$$\frac{\partial H_x}{\partial t} = -\frac{1}{\mu}\frac{\partial E_z}{\partial y} \tag{1a}$$

$$\frac{\partial H_y}{\partial t} = \frac{1}{\mu}\frac{\partial E_z}{\partial x} \tag{1b}$$

$$\frac{\partial E_z}{\partial t} = \frac{1}{\varepsilon}\left(\frac{\partial H_y}{\partial x} - \frac{\partial H_x}{\partial y}\right) - J_z - \sigma E_z \tag{1c}$$

Digital Object Identifier 10.1109/TMAG.2006.871947

where, $\varepsilon, \mu$, and $\sigma$ are the medium permittivity, permeability and conductivity, respectively. is related to the current excitation in the $z$ direction. Applying the CN scheme to approximate the time derivatives in (1), we can obtain the following update [11]–[13]:

$$H_x^{n+1}\left(i,j+\frac{1}{2}\right) = H_x^n\left(i,j+\frac{1}{2}\right) - dbhx\left(i,j+\frac{1}{2}\right) \times\left\{\frac{E_z^{n+1}(i,j+1)-E_z^{n+1}(i,j)+E_z^n(i,j+1)-E_z^n(i,j)}{\Delta y}\right\} \quad (2a)$$

$$H_y^{n+1}\left(i+\frac{1}{2},j\right) = H_y^n\left(i+\frac{1}{2},j\right) + dbhy\left(i,j+\frac{1}{2}\right) \times\left\{\frac{E_z^{n+1}(i+1,j)-E_z^{n+1}(i,j)+E_z^n(i+1,j)-E_z^n(i,j)}{\Delta x}\right\} \quad (2b)$$

$$E_z^{n+1}(i,j) = caez(i,j)E_z^n(i,j) + cbez(i,j). \times\left\{\begin{array}{l}\frac{H_y^{n+1}\left(i+\frac{1}{2},j\right)-H_y^{n+1}\left(i-\frac{1}{2},j\right)+H_y^n\left(i+\frac{1}{2},j\right)-H_y^n\left(i-\frac{1}{2},j\right)}{\Delta x} \\ -\frac{H_x^{n+1}\left(i,j+\frac{1}{2}\right)-H_x^{n+1}\left(i,j-\frac{1}{2}\right)+H_x^n\left(i,j+\frac{1}{2}\right)-H_x^n\left(i\frac{1}{2},j-\frac{1}{2}\right)}{\Delta y}\end{array}\right\} - jez(i,j)J_x^n(i,j) \quad (2c)$$

where the indices $i$ and $j$ refer to the indices of the standard Yee's cell, and the and are the mesh size in the $x$ and $y$ directions respectively. The coefficients in the above equations are given by

$$caez(i,j) = \left(1-\frac{\sigma(i,j)\Delta t}{2\varepsilon(i,j)}\right)/\left(1+\frac{\sigma(i,j)\Delta t}{2\varepsilon(i,j)}\right) \quad (3a)$$

$$cbez(i,j) = \left(\frac{\Delta t}{\varepsilon(i,j)}\right)/2\left(1+\frac{\sigma(i,j)\Delta t}{2\varepsilon(i,j)}\right) \quad (3b)$$

$$dbhx\left(i,j+\frac{1}{2}\right) = \frac{1}{2}\left(\frac{\Delta t}{\mu\left(i,j+\frac{1}{2}\right)}\right) \quad (3c)$$

$$dbhy\left(i+\frac{1}{2},j\right) = \frac{1}{2}\left(\frac{\Delta t}{\mu\left(i+\frac{1}{2},j\right)}\right) \quad (3d)$$

$$\mathrm{jez}(i,j) = \frac{\Delta t}{\varepsilon(i,j)\left(1+\frac{\sigma(i,j)\Delta t}{2\varepsilon(i,j)}\right)}. \quad (3e)$$

Unlike the conventional FDTD method, (2) cannot be updated explicitly since the same time index appears on both sides of equations. We need to use implicit techniques to solve these equations. Substituting (2a) and (2b) into (2c), we can obtain the update equation for (2c) as

$$\begin{aligned}&-c_1\cdot E_z^{n+1}(i+1,j) - c_2\cdot E_z^{n+1}(i-1,j) - c_3\cdot E_z^{n+1}(i,j+1) - c_4\cdot E_z^{n+1}(i,j-1) + \{1+c_1+c_2+c_3+c_4\}E_z^{n+1}(1,j)\\ &\quad = \{caez(1,j)-c_1-c_2-c_3-c_4\}E_z^n(1,j) + c_1\cdot E_z^n(i+1,j) + c_2\cdot E_z^n(i-1,j) + c_3\cdot E_z^n(i,j+1) + c_4\cdot E_z^n(i,j-1)\\ &\quad\quad + cbez(1,j)\cdot\left\{c_5\cdot H_y^n\left(i+\frac{1}{2},j\right) - c_5\cdot H_y^n\left(i-\frac{1}{2},j\right) - c_6\cdot H_x^n\left(i,j+\frac{1}{2}\right) + c_6\cdot H_x^n\left(i,j-\frac{1}{2}\right)\right\}\end{aligned} \quad (4)$$

where

$$\begin{aligned}c1 &= cbez(i,j)dbhy(i+1/2,j)/\Delta x^2,\\ c2 &= cbez(i,j)dbhy(i-1/2,j)/\Delta x^2\\ c3 &= cbez(i,j)dbhx(i,j+1/2)/\Delta y^2,\\ c4 &= cbez(i,j)dbhx(i,j-1/2)/\Delta y^2\\ c5 &= 1/\Delta x \quad \text{and} \quad c6 = 1/\Delta y.\end{aligned}$$

In (4), the field values on the right-hand side of the equation are known prior to updating. The left-hand side of the equation indicates that an element and its neighboring element must be updated at the same time. Applying the CN-FDTD method to all the nodes in the computational domain, we can obtain a system equation for the field update as, where values for elements in the matrix $A$ are determined from the left-hand side of (4) and the values of the vector $b$ are calculated from the right-hand side of (4). The $x$ represents all of the components in the computational space.

### *B. Algebraic Multi-Grid (AMG) Algorithm*

The resulting CN matrix equation can be solved either using the sparse matrix solver or using iterative technique. However, the sparse matrix typically requires an $O(n^2)$ operation if $n$ is the number of unknowns. If an efficient iterative method is used, the number of iterations can be much smaller. Several iterative methods, such as conjugate gradient based techniques, are among popular choices in computational electromagnetics. However, the required number of iterations becomes very large if the simulation time step size increases. This has a detriment effect on the unconditionally algorithms since the purpose of using the unconditionally stable algorithm is to use larger time step sizes while keeping computational overhead minimum. Therefore a more efficient iterative solver must be used.

In this study, the algebraic multi-grid (AMG) method is used to solve the band-limited matrices from the CN-FDTD method. This approach does not require the unknown variables to be defined at known grid points but directly on the given linear sparse algebraic equations [15], such as

$$\mathbf{Au} = \mathbf{b} \text{ or } \sum_{j=1}^{n} a_{\mathrm{ij}}u_j = b_i \quad (i = 1,2,\ldots n).$$

Based on the information given by the matrix itself, one can define all of the necessary components to create an appropriate correction algorithm for AMG: a relaxation scheme, a set of coarse-grid points, a coarse-grid operator, and intergrid transfer operators and. The procedure to construct the two-level correction algorithm can be illustrated as [15]–[17]:

- Step 1) Perform Relaxations on $\mathbf{A}^h\mathbf{u}^h = \mathbf{b}^h$ on the fine-grid $\Omega^h$ with last time step solutions $\mathbf{u}_n^h$ and get the initial new time step solutions $\mathbf{u}_{n+1,\mathrm{odd}}^h$
- Step 2) Compute the fine-grid residual $\mathbf{r}^h = \mathbf{b}^h - \mathbf{A}^h\mathbf{u}_{n+1,\mathrm{odd}}^h$ and restrict it to the coarse grid by.
- Step 3) Solve $\mathbf{A}^{2h}\mathbf{e}^{2h} = \mathbf{r}^{2h}$ on the coarse-grid $\Omega^{2h}$.
- Step 4) Interpolate the coarse-grid error to the fine grid byand improve the fine-grid solutions by $\mathbf{u}_{n+1,\mathrm{new}}^h = \mathbf{u}_{n+1,\mathrm{odd}}^h + \mathbf{e}^h$.

Step 5) $n = n + 1$, go to step 1.

Once the matrix information generated by the CN-FDTD is available, we can apply the AMG method described above to obtain the solution. The AMG technique is used to solve the linear equation described by (4) during each CN-FDTD time stepping.

### C. Maximum Step Size for Practical Simulations

The CN-FDTD method allows us to use time step that is much larger than the conventional FDTD method. However, the algorithm's accuracy is closely related to the simulation time step sizes. In order to maintain a similar numerical accuracy as that of the conventional FDTD method, there is a limit on the maximum time step size that one can use.

The maximum time step size can be derived via the numerical dispersion analysis. Such analysis can be performed using the standard Von Neumann analysis as described in [8], [11], [12]. Through standard dispersion error analysis, we obtain the dispersion relation for the 2D CN-FDTD scheme as

$$\frac{\tan^2(\omega\Delta t/2)}{(c\Delta t)^2} = \frac{\sin^2(k_x\Delta x/2)}{\Delta x^2} + \frac{\sin^2(k_y\Delta y/2)}{\Delta y^2} \quad (5)$$

where $k_x$ and $k_y$ are the wave numbers in the $x$ and $y$ direction respectively, and $k = \sqrt{k_x^2 + k_y^2}$. For comparison purposes, we also give the dispersion relation for the conventional FDTD method as

$$\frac{\sin^2(\omega\Delta t/2)}{(c\Delta t)^2} = \frac{\sin^2(k_x\Delta x/2)}{\Delta x^2} + \frac{\sin^2(k_y\Delta y/2)}{\Delta y^2}. \quad (6)$$

To understand the dispersion error as a function of both sampling rate and simulation time step size, the dispersion error of the CN-FDTD method as a function of the sampling rate and the time step size is shown in Fig. 1. In the figure, the $N_{\text{step}}$ is defined as the ratio of CN-FDTD simulation time step size to the CFL number. The maximum dispersion error is capped at 10%. Each line in the figure corresponds to a constant dispersion error (in percentage). Different sampling rate and $N_{\text{step}}$ can lead to the same dispersion error. As clearly indicated in the figure, the dispersion error increases as the time step size increases and it decreases as the sampling rate increases. It should be pointed out that the maximum allowable time step size is related to the sampling rate. For example, in order to maintain a dispersion error of around 0.5% at each grid point, the maximum time step one can use is about 6 times of the CFL number when the sampling rate is at 100 points per wavelength.

Based on the analyses above, the time step size in the CN-FDTD simulation can be much larger than the conventional FDTD method. Since the maximum time step size allowed by the dispersion error is stricter, we conclude that the CN-FDTD simulation time step sizes should be limited by the maximum allowable time step size imposed by the dispersion error.

## III. Numerical Example

Based on the AMG accelerated CN-FDTD method described in Section 2, a software package is developed for 2D electrically overly-sampled bio-electromagnetic analysis. Before applying the developed software to analyze specific problems, we first validate our software via a numerical example. Here, the electric field strength radiated by a current source as a function of distance away from the source is calculated using the CN-FDTD method and compared with an analytical solution. For this particular verification, the operating frequency is at 1 GHz and the discretization cell size is 0.003 m. Therefore, the sampling rate is at 100 points per wavelength. The time step size we can use here is six times that of the conventional FDTD method. The result from the CN-FDTD simulation and the results from analytical analyses are both shown in Fig. 2. As shown in the figure, they agree well with each other. The minor difference between the numerical results and the analytical solution is caused by the reflection from the absorbing boundary.

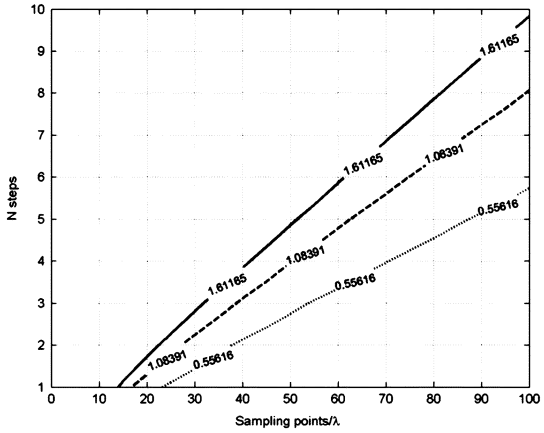


Fig. 1. Appropriate time step size for CN-FDTD simulation as a function of sampling rates at different dispersion error levels (in percentage).

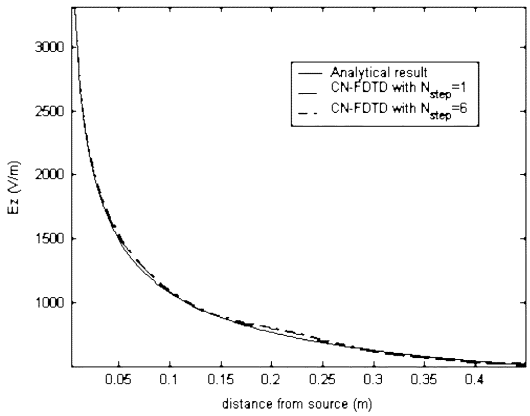


Fig. 2. Comparison between the analytical solution and the CN-FDTD method at different time step sizes.

Once the code is verified, we apply this technique to analyze the induced current distribution within a human head model due to electromagnetic radiation from a hand-held metal detector (HHMD). The HHMD is about 2 cm from the head model and the excitation current is 1 A. The operating frequency of the HHMD is at 8 MHz, and the configuration is shown in Fig. 3. In this simulation, we use $N_{\text{step}} = 160$ and $N_{\text{step}} = 1600$.

In Fig. 4, the layer-averaged induced current along the $y$ axis within the human head model is shown. In the figure, there are two dips close to the peripheries of the head. This is due to the fact that these two dip locations coincide with the bone region, where the electrical conductivities are extremely low. In general,

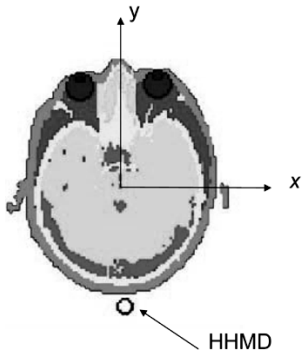


Fig. 3. Configuration of the HHMD simulation.

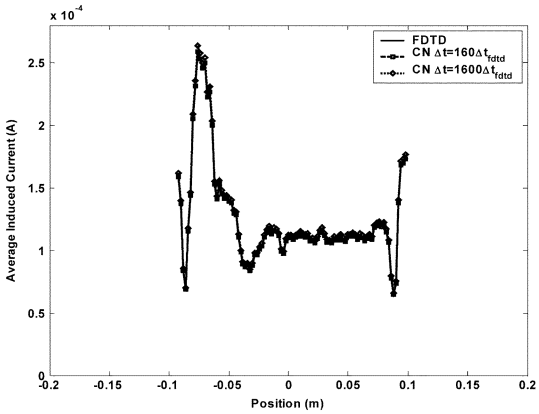


Fig. 4. Layer averaged-induced current along y direction.

the induced current density has a large value close to the head surface region and drops to a low level within the head region. With, the CPU time of the proposed approach is comparable to that of the conventional FDTD method. When is used in this simulation, the CPU time for the proposed approach is about 175 seconds while for the conventional FDTD method it requires 1681 seconds, which is about 10 times longer. A relative error, defined as $(\|E_z^{\mathrm{CN-FDTD}} - E_z^{\mathrm{FDTD}}\|)/(\|E_z^{\mathrm{FDTD}}\| \times 100\%$ is evaluated in the entire computational domain. An average relative error of 1.87% is observed with. It is clear that for electrically overly-sampled biological objects, the proposed approach can dramatically improve the computational efficiency without sacrificing simulation accuracy.

## IV. Conclusion

A multi-grid accelerated CN-FDTD method is proposed for low-frequency bio-electromagnetic simulations. This algorithm is unconditionally stable and yet has very low computational overhead. Numerical examples are used to demonstrate the accuracy and efficiency of this method. For low-frequency electromagnetic applications, this algorithm can be much faster than that of the conventional FDTD method.

**Disclaimer**: The opinions and conclusions stated in this paper are those of the authors and do not represent the official position of the Department of Health and Human Services. The mention of commercial products, their sources, or their use in connection with material reported herein is not to be construed as either an actual or implied endorsement of such products by the Department of Health and Human Services.

## Acknowledgment

This work was supported in part by the National Science Foundation under Grant BES-0332957.

## References

[1] W. Kainz, D. D. Chan, J. P. Casamento, and H. I. Bassen, "Calculation of induced current densities and specific absorption rates (SAR) for pregnant women exposed to hand-held metal detectors," *Phys. Med. Biol.*, vol. 48, pp. 2551–2560, 2000.

[2] J. Chen, Z. M. Feng, and J. M. Jin, "Numerical simulation of SAR and B1-field inhomogeneity of shielded RF coils loaded with the human head," *IEEE Trans. Biomed. Eng.*, vol. 45, no. 5, pp. 650–659, May 1998.

[3] J. Wang, O. Fujiwara, and T. Nojima, "A model for predicting electromagnetic interference of implanted cardiac pacemaker by mobile telephone," *IEEE Trans. Microw. Theory Tech.*, vol. 48, no. 11, pp. 2121–2125, Nov. 2000.

[4] A. Taflove, *Editor Advances in Computational Electrodynamics, The Finite-Difference Time-Domain Method*. Norwood, MA: Artech House, 1998.

[5] C. Furse and O. P. Gandhi, "Calculation of electric fields and currents induced in a millimeter-resolution human model at 60 Hz using the FDTD method," *Bioelectromagnetics*, vol. 19, no. 5, pp. 293–299, 1998.

[6] J. Chen, C. Wu, T. Lo, K.-L. Wu, and J. Litva, "Using linear and nonlinear predictors to improve the computational efficiency of FD-TD algorithm," *IEEE Trans. Microw. Theory Tech.*, no. 10, pp. 1992–1997, Oct. 1994.

[7] T. Namiki, "A new FDTD algorithm based on alternating-direction implicit method," *IEEE Trans. Microw. Theory Tech.*, vol. 47, no. 10, pp. 2003–2007, Oct. 1999.

[8] S. G. Garcia, T. W. Lee, and S. C. Hagness, "On the accuracy of the ADI-FDTD method," *IEEE Antennas Wireless Propag. Lett.*, vol. 1, no. 1, pp. 31–34, 2002.

[9] S. Wang, F. L. Teixeira, and J. Chen, "An iterative ADI-FDTD with reduced splitting error," *IEEE Microw. Wireless Compon. Lett.*, vol. 15, no. 2, pp. 92–94, Feb. 2005.

[10] G. Sun and C. W. Trueman, "Unconditionally stable Crank-Nicolson scheme for solving two-dimensional Maxwell's equations," *Electron. Lett.*, vol. 30, no. 7, pp. 595–597, 2003.

[11] G. D. Smith, *Numerical Solution of Partial Differential Equations: Finite Difference Method*, 2nd ed. Oxford, U.K.: Clarendon, 1978.

[12] W. F. Ames, *Numerical Methods for Partial Differential Equations*. New York: Academic, 1977.

[13] A. R. Mitchell and D. F. Griffiths, *The Finite Difference Method in Partial Differential Equations*. New York: Wiley, 1980.

[14] Y. Saad, *Iterative Methods for Sparse Linear Systems*. New York: PWS, 1996.

[15] W. L. Briggs, V. E. Henson, and S. F. McCormick, *A Multigrid Tutorial*. Philadelphia, PA: SIAM, 2000.

[16] T. Fullenbach and K. Stuben, "Algebraic multigrid for selected PDE systems," in *Proceedings of the 4th European Conference*. London, U.K.: World Scientific, 2002, pp. 399–410.

[17] U. Trottenberg, C. W. Oosterlee, and A. Schuller, *Multrigrid*. San Diego, CA: Academic, 2001.

Manuscript received June 28, 2005 (e-mail: jchen18@uh.edu).